

Properties of antimony doped ZnO thin films deposited by spray pyrolysis technique

© Sadananda Kumar N., Kasturi V. Bangera, G.K. Shivakumar

Thin Films Laboratory, Department of Physics, National Institute of Technology Karnataka, Surathkal, 575025 Mangalore, India.

(Получена 18 сентября 2013 г. Принята к печати 2 декабря 2014 г.)

Antimony (Sb) doped zinc oxide (ZnO) thin films were deposited on the glass substrate at 450°C using spray pyrolysis technique. Effect of Sb doping on surface morphology structural, optical and electrical properties were studied. X-ray diffraction (XRD) analysis showed that both the undoped and doped ZnO thin films are polycrystalline in nature with (101) preferred orientation. SEM analysis showed a change in surface morphology of Sb doped ZnO thin films. Doping results in a marked increase in conductivity without affecting the transmittance of the films. ZnO films prepared with 3 at% Sb shows the lowest resistivity of $0.185 \Omega \cdot \text{cm}$ with a Hall mobility of $54.05 \text{ cm}^2 \text{V}^{-1} \text{s}^{-1}$, and a hole concentration of $6.25 \times 10^{17} \text{ cm}^{-3}$.

1. Introduction

Zinc oxide (ZnO) is one of the most important oxide semiconductors belongs to II–VI group. It has a direct wide band gap (3.37 eV) and high exciton binding energy of 60 meV [1] which makes it a very attractive material for laser emitting devices [2], light emitting diode [3], and field emission devices [4]. Due to the several properties of ZnO, it has applications in the field of solar cells [5], flat panel display [6], heat reflecting mirrors [7], gas sensors [8] and catalysers [9]. ZnO can be used as an alternative candidate to the limited natural resource indium tin oxides (ITO) in the flat panel displays. However, the optical and electrical properties of undoped ZnO do not reach the requirements of high performance semiconductor devices [10]. In order to enhance these properties ZnO should be doped with various dopants.

Doping is a very useful process to enhance the optical and electrical properties of ZnO thin films. Doping of ZnO with Al, In and Ga were widely investigated by various group of researchers [11] and it resulted in *n*-type conductivity. Many research groups attempted to dope ZnO with I group and V group elements [12–14] and to realize the possibility of *p*-type conductivity films. Among these materials doping of antimony is special interest because it is expected to result in the *p*-type conduction by introducing the acceptor levels. The various methods have been used to deposit the pure and doped zinc oxide thin films such as pulsed laser deposition [15], sputtering [16], physical vapour deposition [17], molecular beam epitaxy [18], hydrothermal process [19], chemical vapour deposition [20], sol gel method [21] and spray pyrolysis technique [22]. But spray pyrolysis is one of the simple and convenient technique to deposit the doped and undoped oxide thin films.

In the present study Sb doped ZnO thin films have been deposited by spray pyrolysis technique and effect of Sb doping on the surface morphology, structural, electrical and optical properties of zinc oxide thin films have been studied.

2. Experimental details

Undoped and Sb doped ZnO thin films were deposited on to the glass substrate using spray pyrolysis technique. The starting solution of 0.05M concentrations of zinc acetate anhydrous $[\text{Zn}(\text{CH}_3\text{COO})_2]$ in methanol $[\text{CH}_3\text{OH}]$ was used to spray. Antimony acetate $[\text{Sb}(\text{CH}_3\text{COO})_3]$ is used as a source of dopant, a small amount of which is added to the starting solution. By changing the weight ratio $[\text{Sb}/\text{Zn}]$ the doping level is varied. The glass substrates were kept in concentrated nitric acid for 24 h to remove the surface impurities present on it. After removing the glass substrate, it is washed with soap solution, further it is cleaned with acetone, isopropyl alcohol and finally with deionised water using ultrasonic bath and dried. During deposition the temperature was maintained at $450 \pm 5^\circ\text{C}$, the spray nozzle is fixed at a distance of 24 cm from the substrate, the solution is sprayed at the rate of 2 ml/min. Air is used as carrier gas at the pressure of 0.2 Torr. Pyrolytic process occurs, when the aerosol droplets reach the hot glass substrate and adherent films were produced.

The thickness of the deposited film was measured by gravimetric method and the films of 600 nm thickness were used in the present study. The structural characterization of the film was carried out using X-ray diffractometer (XRD), with $\text{Cu } k_\alpha$ radiation of wavelength $\lambda = 1.5418 \text{ \AA}$. The influence of Sb dopant on the structure of ZnO thin films was investigated. Scherrer's method was used to calculate the average crystallites size of the films. Scanning electron microscope (SEM) has been used to record the surface micrographs of Sb doped ZnO thin films. $[\text{Sb}/\text{Zn}]$ ratio in the ZnO films is determined using the energy dispersive analysis of X-ray's (EDAX). The optical measurements of undoped and Sb doped ZnO thin films were carried out using UV — Visible spectrophotometer in the wavelength range of 200–900 nm at room temperature. The electrical characteristics of the films were studied using Keithley source meter and multimeter. The Hall measurements of the Sb doped films were examined by using Van-der-Pauw

† E-mail: sadanthara@gmail.com

method at room temperature in a magnetic field strength of 0.3 T.

3. Results and discussions

3.1. Structural & morphological characterization

XRD studies have been performed to investigate the structure of undoped and Sb doped ZnO thin films. Fig. 1 shows the XRD pattern of undoped and Sb doped ZnO thin films. Both the undoped and Sb doped films exhibit hexagonal wurtzite polycrystalline structure. The undoped ZnO thin films have preferred orientation along (002) direction, with the intensities of other peaks being relatively low. Sb doped ZnO thin films show a preferred orientation along (101) direction. Further, it is observed that with increase in the concentration of dopant, the intensity corresponding to the (101) set of planes decreases. Shift in the peak positions is used to compute the changes in the lattice parameter of the films. It is observed that doping does not result in changes in lattice parameter indicates no lattice distortion. There is no peak corresponding to free antimony or related compound detected in the XRD pattern.

The crystal quality of the ZnO thin films are decided by the crystallites size calculated from measurements on the peak in the diffraction pattern. The crystallites size (D) in the film was determined using the Scherrer's formula [23]

$$D = 0.9\lambda / \beta \cos \theta, \quad (1)$$

where D is the crystallite size, λ is the wavelength, β is the full width at half maximum (FWHM) of the peak and θ the Bragg angle. The estimated crystallite size was found to be in the range 15 to 20 nm indicates fine grain structure for the films. This is further compared with SEM images of the films (Fig. 2). The grain size is found to decreases marginally for films doped with 5% Sb (Table 1).

The lattice parameters 'a' and 'c' of undoped and Sb doped ZnO thin films were calculated using the formula [23]

$$1/d^2 = 4(h^2 + k^2 + hk)/3a^2 + l^2/c^2, \quad (2)$$

where d is the interplaner separation h, k, l are crystal plane index, a, b and c are lattice parameters, respectively. The calculated values of „a“ and „c“ matched well with reported data [JCPDS file No. 080–0074 ($a = 3.2535 \text{ \AA}$, $c = 5.2151 \text{ \AA}$)]. This clearly indicates the incorporation of Sb in the ZnO lattice does not distort the lattice.

Table 1. XRD data of undoped and Sb doped ZnO thin films

Sb, at%	Orientation	D , nm	a , Å	c , Å
0	(002)	15.3	3.23	5.23
1	(101)	15.9	3.26	5.23
3	(101)	18.9	3.25	5.22
5	(101)	13.9	3.25	5.22

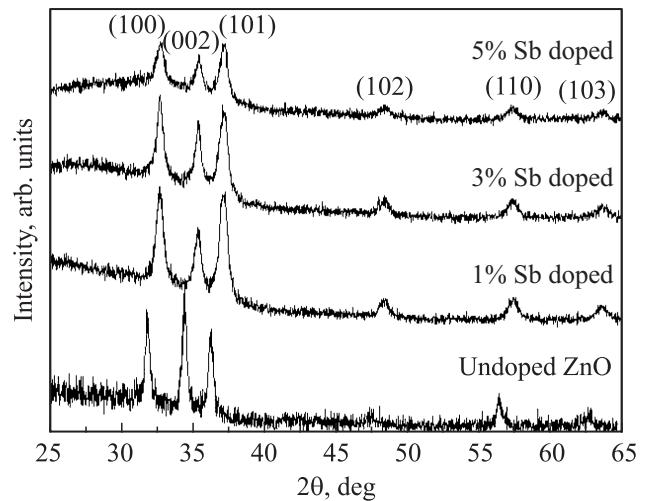


Figure 1. XRD pattern of undoped and Sb doped ZnO thin films.

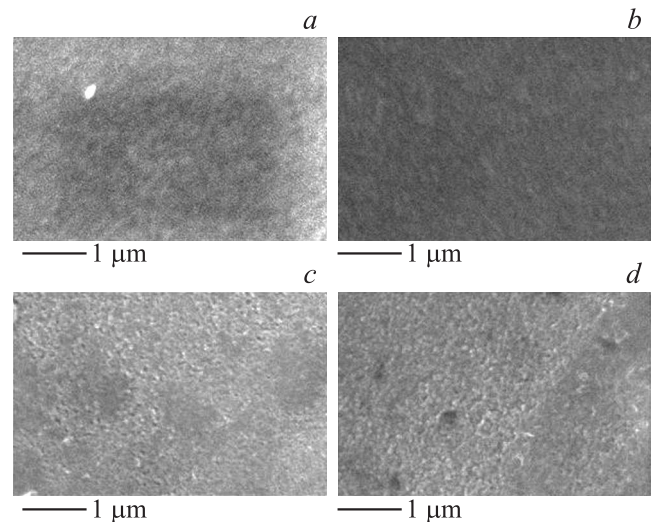


Figure 2. SEM images of (a) undoped ZnO, (b) 1 at% Sb doped (c) 3 at% Sb doped and (d) 5 at% Sb doped ZnO thin films.

The scanning electron micrographs of undoped and Sb doped ZnO films were shown in Fig. 2. The successful incorporation of Sb in the ZnO lattice was confirmed by EDAX analysis.

3.2. Optical characterization

The effect of concentration of Sb dopant on the optical transmittance (T) and energy band gap of ZnO thin films has been studied. Transmittance spectra of undoped and Sb doped ZnO thin films are presented in the Fig. 3. It is found that, all the films have the transmittance above 75% in the visible region and sharp absorption edge in the UV region. This indicates that the Sb dopant do not affect the transmittance of the film. The sharp decrease in the transmission near UV region was observed due to the band gap absorption. Good transmittance in the visible region

reveals that films has less defects and better crystallinity [24]. It is observed that the absorption edge of Sb doped ZnO thin films shifts to lower wavelength region when compared with undoped ZnO thin films. Using absorption data, absorption coefficient (α) is calculated to obtain the band gap values with the help of following relation [25]

$$\alpha = \ln(1/T)/t, \tag{3}$$

where T is the transmittance, t is the thickness of the film. Furthermore there are no interference effects in transmission spectra indicating the uniformity of surface and small crystallites size. The undoped as well as Sb doped ZnO thin films have a direct band gap. For the direct allowed transition, the band gap of ZnO thin films can be determined using the relation [26]

$$(\alpha h\nu) = A(h\nu - E_g)^{1/2}, \tag{4}$$

where A is constant, $h\nu$ is photon energy and E_g is the energy band gap.

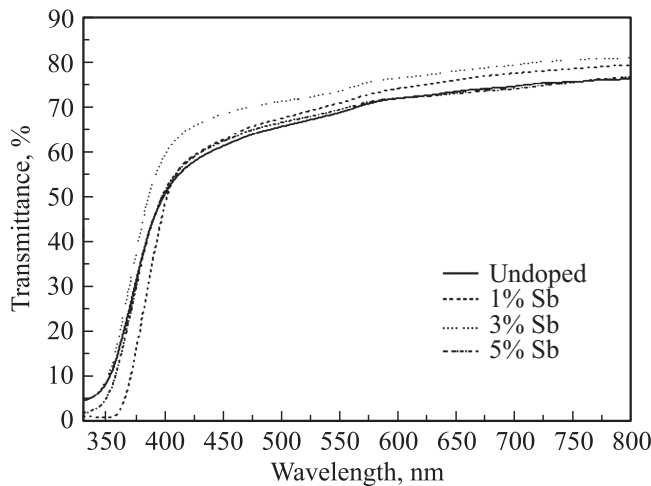


Figure 3. Transmittance spectra of undoped and Sb doped ZnO thin films.

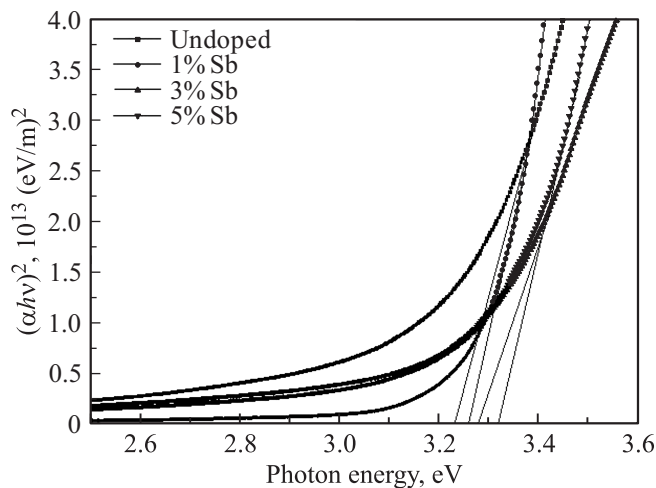


Figure 4. Variation of $(\alpha h\nu)^2$ versus $h\nu$ of undoped and Sb doped ZnO thin films.

Table 2. The optical and electrical data of undoped and Sb doped ZnO thin films

Sb, at%	T , %	E_u , meV	E_g , eV	σ , S · cm	E_a , meV
0	78	–	3.24	0.156	348 –
1	79	469	3.26	0.532	441 50
3	75	415	3.28	5.4	444 54
5	75	357	3.32	4.67	373 69

Fig. 4 shows the variation of $(\alpha h\nu)^2$ with $h\nu$ for undoped and Sb doped ZnO thin films. The extrapolation of linear part of $(\alpha h\nu)^2$ versus $h\nu$ plot to the x -axis gives the energy band gap (E_g) of the film. The linear part in the plot indicates the direct allowed transition [26]. The energy band gap value obtained for undoped ZnO thin film is 3.24 eV. The variations of optical band gap with concentration of Sb dopant are presented in Fig. 4. It is found that E_g values slightly increased from 3.24 to 3.34 eV as the concentration of dopant increased from 0 to 5 at%. Widening of the energy band gap may be explained on the basis of Moss–Burstein theory [27]. According to the theory, in heavily doped zinc oxide films, the donor electrons occupy states at the bottom of the conduction band. Since the Pauli’s principle prevents states from being doubly occupied and optical transitions are vertical, the valence electrons require an additional energy to be excited to higher energy states in the conduction band. Therefore, E_g of doped zinc oxide is broader than that of undoped zinc oxide films [28]. The optical transition between the occupied state in the valence band tail and unoccupied state in the conduction band edge is explained by the following equation

$$\alpha = \alpha_0 \exp(h\nu/E_u), \tag{5}$$

where α_0 is a constant, E_u is the Urbach energy which characterizes the slope of the exponential edge. The values of E_u were obtained from the inverse of the slope of $\ln \alpha$ with $h\nu$ plot and the calculated values are given in the Table 2. The Urbach energy of undoped ZnO is found to be 252.7 meV. It is observed that Urbach energy of Sb doped ZnO films decreases with increasing dopant concentration from 1 to 5 at%. This may be due to the dopant element changes the width of localized state in the optical band. It is noted that Urbach energy value changes inversely with optical band gap [29].

3.3. Electrical characterization

The current–voltage (I – V) characteristics of undoped and Sb doped ZnO thin films were recorded using the two-probe method. Silver is used as a contact material. The measurements have been taken for voltage ranging from -5 V to $+5$ V. Fig. 5 shows the variation of current with voltage. I – V characteristics of doped and undoped ZnO films found to be linear, indicating ohmic conduction

Table 3. Hall measurement data of undoped and Sb doped ZnO films

Sample	Resistivity, ρ ($\Omega \cdot \text{cm}$)	Carrier concentration, n (cm^{-3})	Mobility, μ ($\text{cm}^2\text{V}^{-1}\text{s}^{-1}$)	Conduction type
Undoped	6.41	$9.92 \cdot 10^{16}$	9.38	<i>n</i>
1at% Sb	1.88	$3.57 \cdot 10^{17}$	9.30	<i>n</i>
3 at% Sb	0.185	$6.25 \cdot 10^{17}$	54.05	<i>p</i>
5 at% Sb	0.214	$6.51 \cdot 10^{17}$	44.72	<i>p</i>

mechanism. It is found that the conductivity of ZnO thin films varies with the addition of Sb dopant.

The variation in the electrical conductivity (σ) of ZnO thin films with the concentration of Sb dopant is shown in Fig. 6. It is noted that the conductivity of ZnO films increases up to 3 at% addition of Sb. This may be due to replacement of Zn^{2+} by Sb^{3+} , contributing additional charge carriers to the electrical conduction. Thus increase in the electrical conductivity may be attributed to the presence of large number of charge carriers introduced by the dopant [30]. Decrease in the conductivity of 5 at% Sb doped ZnO films may be due to disorder produced in the ZnO lattice, which leads the scattering of carriers such as ionised impurity scattering or phonon scattering. The high conductivity of 5.4 Scm^{-1} was obtained for 3 at% Sb doped ZnO films. This result is consistent with structural result that maximum crystallite size and minimum dislocation density for 3 at% Sb doping.

The *p*-type conductivity of Sb doped ZnO materials have been reported by group of researchers [31,32]. According to Limpijumnonng et al. [33] $\text{Sb}_{\text{Zn}}-2\text{V}_{\text{Zn}}$ complex was most likely candidate to form a shallow acceptor level in large-sized mismatched group-V-doped ZnO. The *n*-type conductivity is observed in the 1 at% Sb doped films. This is due to low concentration of dopant which is not enough to change the conductivity from *n*-type to *p*-type. Although Sb_{Zn} is produced in the film, the concentration of $\text{Sb}_{\text{Zn}}-2\text{V}_{\text{Zn}}$ complex is too small to show *p*-type conductivity. On increasing the doping concentration to 3 and 5 at% the formation of $\text{Sb}_{\text{Zn}}-2\text{V}_{\text{Zn}}$ complex is sufficient to flip the conductivity from *n*-type to *p*-type. Table 3 gives the Hall measurement data of undoped and Sb-doped ZnO thin films grown at different doping concentrations. It is observed that *p*-type conduction can be achieved above a concentration of 3 at% Sb dopant. It is worth noting that the films prepared with 3 at% Sb shows the low resistivity of $0.185 \Omega\text{-cm}$ with a Hall mobility of $54.05 \text{ cm}^2\text{V}^{-1}\text{s}^{-1}$, and a hole concentration of $6.25 \times 10^{17} \text{ cm}^{-3}$.

The variation of resistance with temperature of the Sb doped ZnO films has been studied. Fig. 6 shows a plot of $\log R$ versus inverse temperature for 3 at% Sb doped ZnO thin film. It is observed that electrical resistivity decreases as the concentration of Sb dopant increases up to 3 at%, since crystallites size increases with doping (Table 2). This diminishes the grain boundary scattering by decreasing the number of grain boundaries. With increasing temperature, resistance of the film decreases

linearly, indicating semiconducting nature of undoped and Sb doped ZnO films. Thus activation energy (E_a) can be calculated from the slope of $\log R$ versus $1/T$ plot. The plot of $\log R$ versus inverse temperature of undoped films shows the single activation energy, whereas Sb doped films show two activation energies at the 2 region of temperature. These activation energies represent shallow and deep donor levels in the films. The double activation energy in the doped ZnO films is also reported by Jimenez–Gonzalez et al. [34] in their Al doped ZnO films prepared by sol gel technique.

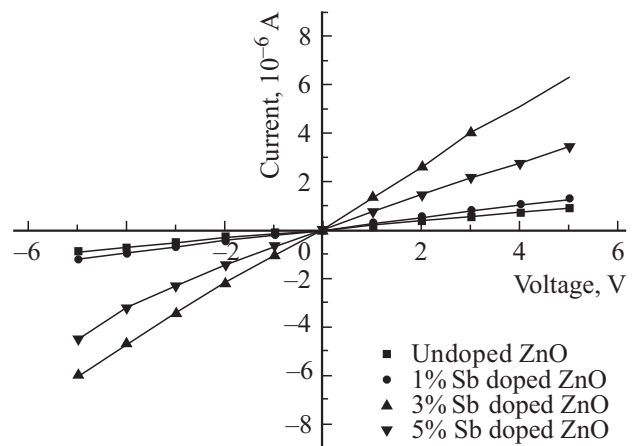


Figure 5. I–V characteristics of undoped and Sb doped ZnO thin films.

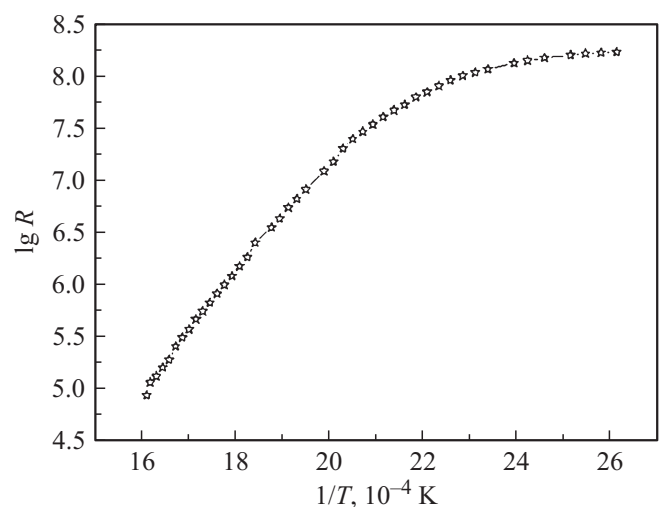


Figure 6. Variation of $\log R$ with $1/T$ of Sb doped ZnO thin films.

Thus the charge carriers in the ZnO films increases by antimony doping and trapping levels with activation energy less than 55 meV contribute to the electrical conductivity with very low energy cost [34]. The calculated values of activation energies are listed in the Table 2.

4. Conclusions

Sb doped ZnO thin films have been deposited on glass substrate using spray pyrolysis technique. The effect of Sb doping on the structural, optical and electrical properties of ZnO thin films has been investigated. XRD analysis reveals that Sb doped ZnO thin films exhibit hexagonal wurtzite structure with (101) preferred orientation. Films doped with 3 at% Sb showed optimum characteristics of high transparency and high electrical conductivity suitable for conducting electrodes.

References

- [1] D.C. Look. Mater. Sci. Eng. B **80**, 383 (2001).
- [2] M.H. Haung, S. Mao, H. Feick. Science, **292**, 1899 (2001).
- [3] Sang Yeol Lee, Eun Sub Shim, Hong Seong Kang, Seong Sik Pang, Jeong Seok Kang. Thin Sol. Films, **473**, 34 (2005).
- [4] R. Maity, A.N. Banerjee, K.K. Chattopadhyay. Appl. Surf. Sci., **236**, 231 (2004).
- [5] S. Fay, J. Steinhauser, N. Oliveira, E. Vallat-Sauvain, C. Ballif. Thin Sol. Films, **515**, 8558 (2007).
- [6] Young Ran Park, Eung Kwon Kim, Donggeun Jung, Tae Seok Park, Young Sung Kim. Appl. Surf. Sci., **254**, 2250 (2008).
- [7] Li Gong, Zhizhen Ye, Jianguo Lu, Liping Zhu, Jingyun Huang, Xiuquan Gu, Binghui Zhao. Vacuum, **84**, 947 (2010).
- [8] H.J. Lim, D.Yong, Y.J. Oha. Sensors Actuators A, **125**, 405 (2006).
- [9] M. Miki-Yoshida, V. Collins-Martinez, P. Amezcaga-Madrid, A. Aguilar-Elguezabal. Thin Sol. Films, **419**, 60 (2002).
- [10] Chien-Yie Tsaya, Kai-Shiung Fana, Sih-Han Chena, Chia-Hao Tsai. J. Alloys Comp., **495**, 126 (2010).
- [11] Chae-Seon Hong, Hyeong-Ho Park, Jooho Moon, Hyung-Ho Park. Thin Sol. Films, **515**, 957 (2006).
- [12] Amit Kumar, Manoj Kumar, Beer Pal Singh. Appl. Surf. Sci., **256**, 7200 (2010).
- [13] Soumen Dhara, P.K. Giri. Thin Sol. Films, **520**, 5000 (2012).
- [14] B.L. Zhu, C.S. Xie, J. Wu, D.W. Zeng, A.H. Wang, X.Z. Zhao. Mater. Chem. Phys., **96**, 459 (2006).
- [15] Xinhua Pan, Zhizhen Ye, Jiesheng Li, Xiuquan Gu, Yujia Zeng, Haiping He, Liping Zhu, Yong Che. Appl. Surf. Sci., **253**, 5067 (2007).
- [16] T. Yang, B. Yao, T.T. Zhao, G.Z. Xing, H. Wang, H.L. Pan, R. Deng, Y.R. Sui, L.L. Gao, H.Z. Wang, T. Wuc, D.Z. Shen. J. Alloys Comp., **509**, 5426 (2011).
- [17] G. Jimenez-Cadena, E. Comini, M. Ferroni, A. Vomiero, G. Sberveglieri. Mater. Chem. Phys., **124**, 694 (2010).
- [18] Min Su Kim, Do Yeob Kim, Min Young Cho, Giwoong Nam, Soaram Kim, Dong-Yul Lee, Sung-O Kim, Jae-Young Leem. Vacuum, **86**, 1373 (2012).
- [19] Xuan Fang, Jinhua Li, Dongxu Zhao, Binghui Li, Zhenzhong Zhang, Dezhen Shen, Xiaohua Wang, Zhipeng Wei. Thin Sol. Films, **518**, 5687 (2010).
- [20] Q.J. Feng, L.Z. Hub, H.W. Liang, Y. Feng, J. Wang, J.C. Sun, J.Z. Zhao, M.K. Li, L. Dong. Appl. Surf. Sci., **257**, 1084 (2010).
- [21] H. Benelmadjat, N. Touka, B. Harieche, B. Boudine, O. Halmi, M. Sebais. Optical. Mater., **32**, 764 (2010).
- [22] T.V. Vimalkumar, N. Poornima, K.B. Jinesh, C. Sudha Kartha, K.P. Vijayakumar. Appl. Surf. Sci., **257**, 8334 (2011).
- [23] W.W. Zhong, F.M. Liu, L.G. Cai, C.C. Zhou, P. Ding, H. Zhang. J. Alloys Comp., **499**, 265 (2010).
- [24] M. Rusop, K. Uma, T. Soga, T. Jimbo. Mater. Sci. Eng. B, **127**, 150 (2006).
- [25] T. Prasada Rao, M.C. Santhoshkumar. Appl. Surf. Sci., **255**, 4579 (2009).
- [26] U. Alver, T. Kılınc, E. Bacaksız, T. Kucukomeroglu, S. Nezir, I.H. Mutlu, F. Aslan. Thin Sol. Films, **515**, 3448 (2007).
- [27] Anubha Jain, P. Sagar, R.M. Mehra. Sol. St. Electron., **50**, 1420 (2006).
- [28] F. Chouikh, Y. Beggah, M.S. Aida. J. Mater. Sci.: Mater. Electron, **22**, 499 (2011).
- [29] Yasemin Caglar, Saliha Ilican, Mujdat Caglar, Fahrettin Yakuphanoglu. Spectrochim. Acta, pt A, **67**, 1113 (2007).
- [30] B.L. Zhu, C.S. Xie, J. Wu, D.W. Zeng, A.H. Wang, X.Z. Zhao. Mater. Chem. Phys., **96**, 459 (2006).
- [31] Xinhua Pan, Zhizhen Ye, Jiesheng Li, Xiuquan Gu, Yujia Zeng, Haiping He, Liping Zhu, Yong Che. Appl. Surf. Sci. **253**, 5067 (2007).
- [32] K. Samanta, A.K. Arora, S. Hussain, S. Chakravarty, R.S. Katiyar. Current Appl. Phys., **12**, 1381 (2012).
- [33] S. Limpijumnong, S.B. Zhang, S.H. Wei, C.H. Park. Phys. Rev. Lett., **92**, 155 504 (2004).
- [34] A.E. Jimenez-Gonzalez, Jose A. Soto Urueta, R. Suarez-Parra. J. Cryst. Growth., **192**, 430 (1998).

Редактор Т.А. Полянская